Review of Active Power Decoupling Topologies in Single-Phase Systems

Yao Sun, *Member, IEEE*, Yonglu Liu, Mei Su, Wenjing Xiong, and Jian Yang, *Member, IEEE*

***Abstract*—Active power decoupling methods are developed to deal with the inherent ripple power at twice the grid frequency in single-phase systems generally by adding active switches and energy storage units. They have obtained a wide range of applications, such as photovoltaic (PV) systems, light-emitting diodes (LEDs) drivers, fuel cell (FC) power systems, and electric vehicle (EV) battery chargers, etc. This paper provides a comprehensive review of active power decoupling circuit topologies. They are categorized into two groups in terms of the structure characteristics: independent and dependent decoupling circuit topologies. The former operates independently with the original converter, and the latter, however, shares the power semiconductor devices with the original converter partially and even completely. The development laws for the active power decoupling topologies are revealed from the view of "duality principle," "switches sharing," and "differential connection." In addition, the exceptions and special cases are also briefly introduced. This paper is targeted to help researchers, engineers, and designers to construct some new decoupling circuit topologies and properly select existing ones according to the specific application.**

***Index Terms*—Active power decoupling, duality principle, photovoltaic (PV) systems, single-phase systems, twice ripple power.**

I. Introduction

SINGLE-PHASE power electronics systems are widely used in low-power applications [1]. Unfortunately, the inherent twice ripple power results in undesirable low-frequency ripple on dc-link voltage/current. The undesirable ripple degrades system performance, for example, reducing the maximum power point tracking (MPPT) efficiency of the photovoltaic (PV) panels [2], leading to light flicker in light-emitting diode (LED) lighting applications [3]–[5], causing overheating of batteries [6], [7], and shortening fuel cell's lifetime [8], [9].

Addressing this issue, the solutions are mainly divided into two categories: passive decoupling method and active decoupling method. The passive decoupling method includes two types: increasing the dc-link inductance or capacitance [10] and making use of *LC* resonant filter [11], [12]. They are easy to implement, but large volume and weight are undesirable from the cost and practicability perspective. Moreover, the life expectancy of large aluminum electrolytic capacitors is limited [13], [14]. The fundamental idea of active decoupling method is to divert the ripple power to another specific energy storage component with relatively small size and long lifetime by an extra active switching circuit. Then, the aforementioned disadvantages of the passive decoupling method are eliminated. Therefore, the requirements for volume-critical and weight-critical applications, such as onboard electrical vehicles [15] and aircraft power systems, as well as lifetime-critical applications, such as PV generation systems [2] and LED lighting systems [3]–[5], are met. Therefore, active decoupling method has attracted much attention in recent years and been studied in various applications.

The active decoupling method consists of control algorithms and decoupling circuit topologies. The control algorithms are mainly divided into the open-loop control method [15]–[77] and the closed-loop control method [78]–[80]. The former is simple to implement, so it is widely used in many literatures. However, it is sensitive to the parameters variation. The closed-loop control could achieve good performance even in the presence of various disturbances, but the design of a stable closed-loop control algorithm is not easy sometimes.

Usually, the decoupling circuit topologies consist of basic decoupling cells and original converters. In some of them, basic decoupling cells and original converters work independently [15]–[51], [78]. In some other cases, basic decoupling cells share switches with original converters partially [52]–[63], [79] and even completely [64]–[69], [80]. As a result, the shared switches work coordinately to achieve the goal of power decoupling as well as power conversion. Besides, there are some decoupling circuit topologies formed by the differential concept [70]–[77].

This paper provides a comprehensive survey on the topic of active power decoupling circuit topologies for single-phase power converters. Different from the review in [2], which presented a comprehensive review of the power decoupling techniques for microinverters in PV application, this paper mainly focuses on the development and construction laws of decoupling topologies.

Section II explains the operating principle of the active power decoupling method. Section III introduces the basic decoupling cells. Sections IV and V describe independent and dependent decoupling topologies, respectively. Special cases are presented in Section VI. Finally, Section VII draws the conclusion.

Manuscript received May 26, 2015; revised June 26, 2015 and August 23, 2015; accepted September 7, 2015. Date of publication September 10, 2015; date of current version January 28, 2016. This work was supported by the National Natural Science Foundation of China under Grant 61573382, the National High-tech R&D Program of China under Grant 2012AA051601, the Hunan Provincial Natural Science Foundation of China under Grant 14JJ5035, and the Project of Innovation-driven Plan in Central South University under Grant 2015CXS006. Recommended for publication by Associate Editor K. Ngo.

The authors are with the School of Information Science and Engineering, Central South University, Changsha 410083, China (e-mail: yaosuncsu@gmail.com; liuyonglu@csu.edu.cn; sumeicsu@mail.csu.edu.cn; csu.xiong@163.com; fish2bear@gmail.com).

Color versions of one or more of the figures in this paper are available online at http://ieeexplore.ieee.org.

Digital Object Identifier 10.1109/TPEL.2015.2477882

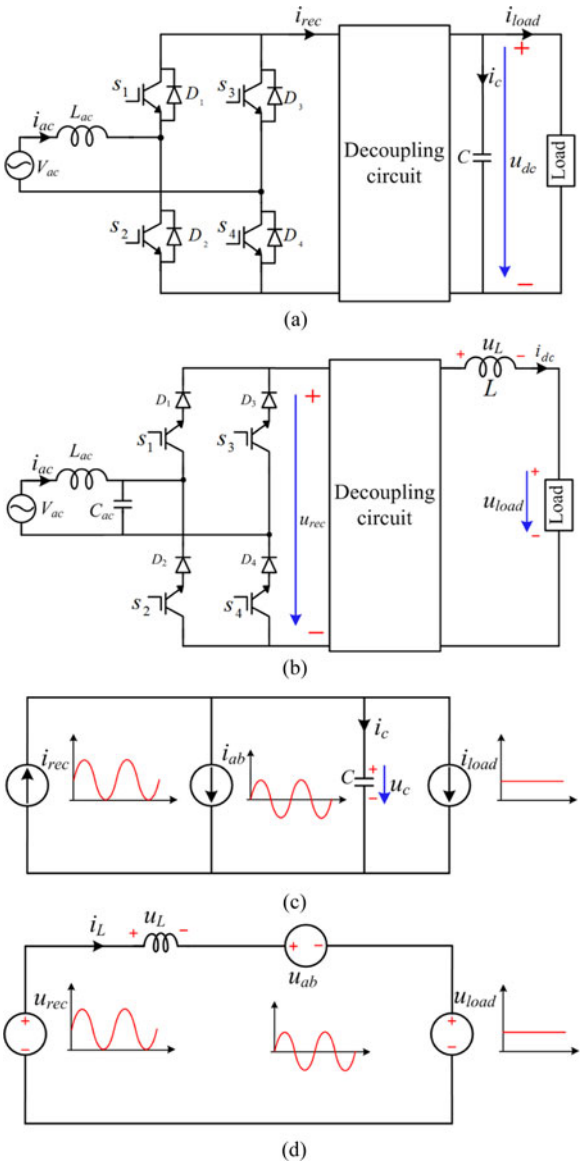

Fig. 1. VSC and CSC configured with a decoupling circuit. (a) Main circuit for VSC. (b) Main circuit for CSC. (c) Equivalent circuit of (a). (d) Equivalent circuit of (b).

II. Operating Principle of the Active Power Decoupling Method

Two classic single-phase voltage-source converter (VSC) and current-source converter (CSC) with active power decoupling circuits are shown in Fig. 1(a) and (b). They are taken for examples to explain the fundamental operation principle of the active power decoupling method.

Assume that the grid voltage $v_{\rm ac}$ and current $i_{\rm ac}$ are sinusoidal, and are expressed as follows:

$$v_{\rm ac} = V\cos(\omega t) \tag{1}$$

$$i_{\rm ac} = I\cos(\omega t + \varphi) \tag{2}$$

where V and I are the amplitudes of the gird voltage and current, ω is grid frequency, and φ is the displacement angle. Then, the instantaneous power $p_{\rm ac}$ of the grid is expressed as

$$p_{\rm ac} = v_{\rm ac} i_{\rm ac} = \underbrace{VI\cos(\varphi)/2}_{P_o} + \underbrace{VI\cos(2\omega t + \varphi)/2}_{P_r} \tag{3}$$

where P_o is the average power, i.e., the load power. P_r is the ripple power, which should be buffered by the decoupling circuit.

For simplicity, the effects of power losses and input filters are neglected. When the decoupling circuits are disabled, according to power balance, the rectified output current $i_{\rm rec}$ of the VSC and output voltage $u_{\rm rec}$ of the CSC are expressed as follows:

$$\begin{aligned} i_{\rm rec} &= v_{\rm ac} i_{\rm ac}/u_{\rm dc} \\ &= \underbrace{0.5VI\cos(\varphi)/u_{\rm dc}}_{i_{\rm load}} + \underbrace{0.5VI\cos(2\omega t + \varphi)/u_{\rm dc}}_{i_r} \end{aligned} \tag{4}$$

$$\begin{aligned} u_{\rm rec} &= v_{\rm ac} i_{\rm ac}/i_{\rm dc} \\ &= \underbrace{0.5VI\cos(\varphi)/i_{\rm dc}}_{u_{\rm load}} + \underbrace{0.5VI\cos(2\omega t + \varphi)/i_{\rm dc}}_{u_r} \end{aligned} \tag{5}$$

where $u_{\rm dc}$ and $i_{\rm dc}$ are the dc-link voltage of the VSC and the dc-link current of the CSC, respectively. When $u_{\rm dc}$ and $i_{\rm dc}$ are controlled to be constant, i_r and u_r will become the sources of the twice ripple power.

Referring to Fig. 1(a) and (b), the dynamics equations of the dc link are

$$C\frac{du_{\rm dc}}{dt} = i_{\rm rec} - i_{\rm load} \tag{6}$$

$$L\frac{di_{\rm dc}}{di} = u_{\rm rec} - u_{\rm load}. \tag{7}$$

To realize perfect constant dc-link voltage/current outputs, according to (6) and (7), infinite value of *C*/*L* is needed, and that is the reason why the passive decoupling method results in an energy storage component with large volume and weight.

If the decoupling circuit shown in Fig. 1(a) is activated, its equivalent circuit is shown in Fig. 1(c). According to Kirchhoff's current law, if i_{ab} takes the value of i_r, the goal of the power decoupling will come true. Similarly, the corresponding equivalent circuit of the CSC with activating the decoupling circuit is shown in Fig. 1(d). According to Kirchhoff's voltage law, if u_{ab} is equal to u_r, the power decoupling will be realized. Because large fluctuation range of the energy storage component in the decoupling circuit is allowed, a much smaller energy storage unit is required compared to the passive decoupling solution The comparisons of the required passive components were carried out in [27], [81], and [82] with/without the active power decoupling circuit. The power density is increased by approximately 50% in [27] and [81] when adopting the active decoupling method.

III. Basic Decoupling Cells

The aim of this section is to introduce the basic decoupling cells and pave the way for the following sections. Basic decoupling cells are the modules which are able to buffer the ripple power. They can be connected to the original converters in series, parallel, or other ways. According to the scope of

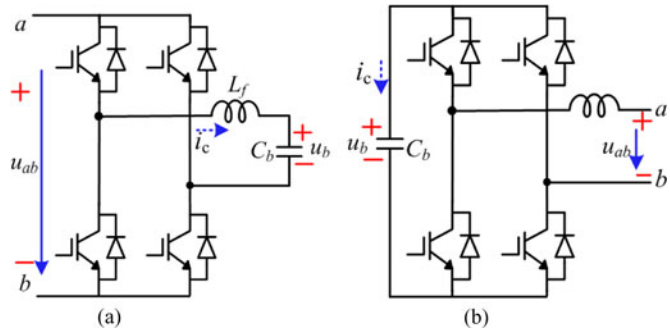

Fig. 2. H-bridge basic decoupling cell with a capacitor as the energy storage unit. (a) With alternative capacitor voltage and dc terminal voltage. (b) With alternative terminal voltage and dc capacitor voltage.

applications, they can mainly be categorized into two groups: the voltage-source-oriented basic cells and the current-source-oriented basic cells; and both of them can be further divided into two types: capacitive energy storage and inductive energy storage.

A. *Voltage-Source-Oriented Basic Decoupling Cells*

1) Capacitive Energy Storage: Recently, the capacitive energy storage has been paid more attention due to the factors such as volume and cost compared to the inductive energy storage. For the capacitive energy storage, the ripple energy is stored in the electrostatic field of capacitors. Fig. 2 shows two kinds of voltage-source-oriented basic decoupling cells. Both of them have the same H-bridge structure but different features. The decoupling capacitor C_b in Fig. 2(a) could withstand alternative voltages. However, the absolute value of the capacitor voltage must be lower than the dc terminal voltage u_{ab}. Usually, to buffer the twice ripple power, the waveforms of the capacitor voltage and current are controlled as illustrated in Fig. 3(a). The decoupling capacitor in Fig. 2(b) could only withstand a dc voltage which must be higher than the corresponding terminal voltage u_{ab}. Under normal condition, its corresponding waveforms are shown in Fig. 3(b). Therefore, considering the same operation condition, the basic decoupling cell in Fig. 2(a) has low voltage stress but needs a capacitor with relatively large capacitance, while the basic decoupling cell in Fig. 2(b) has to suffer high voltage stress but only needs a capacitor with relatively small capacitance.

In fact, if the capacitor of the basic cell in Fig. 2(a) is a polarized capacitor, the basic cell can be reduced to a buck-type decoupling cell as shown in Fig. 4(a). Due to the voltage polarity constraint, the possible waveforms of the capacitor in the buck-type basic decoupling cell are shown in Fig. 3(c) and (d). It is clear that the voltage across the energy storage capacitor in Fig. 3(c) is not as smooth as that in (d). From the view point of control, the waveforms in Fig. 3(c) are more difficult to realize than those in Fig. 3(d). However, the capacity of the energy storage capacitor can be utilized fully in Fig. 3(c).

Similarly, if the terminal voltage u_{ab} of the basic cell in Fig. 2(b) is a dc voltage, then the basic cell can be reduced to the

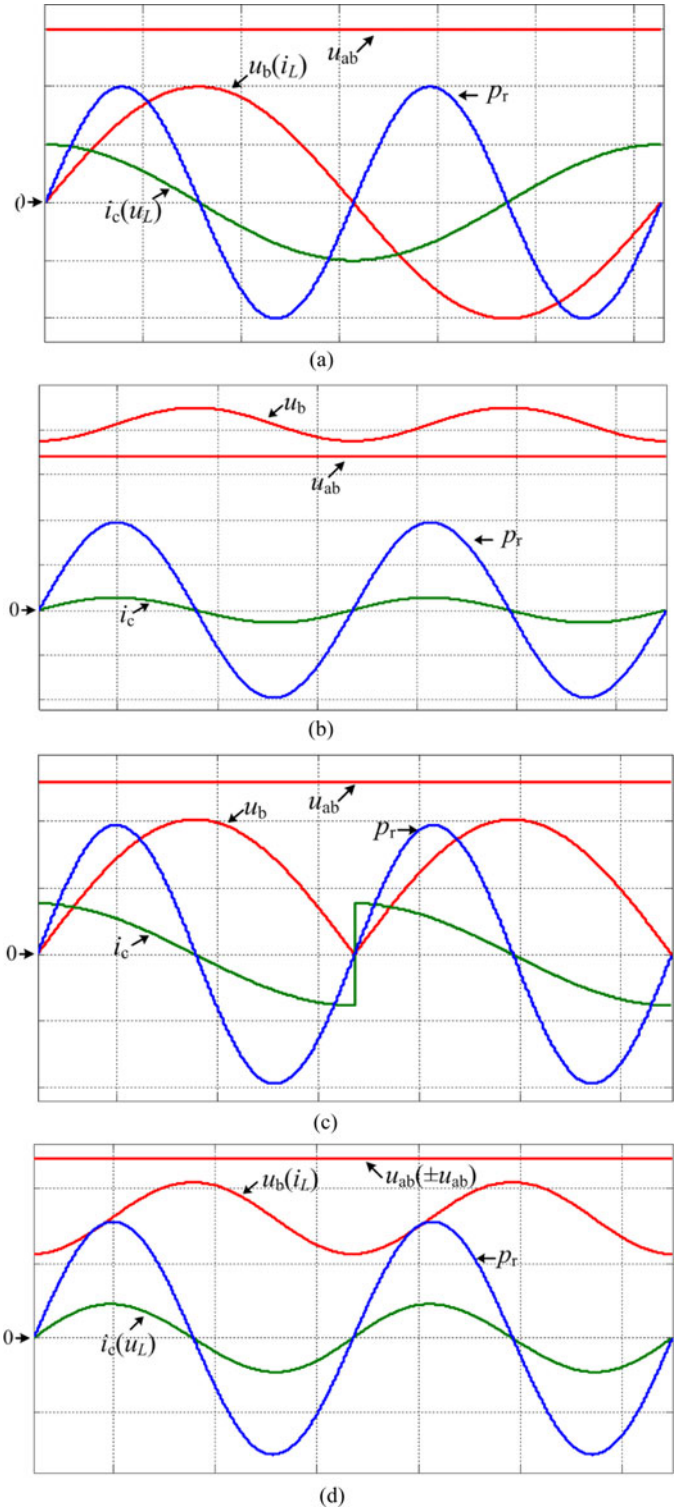

Fig. 3. Waveforms of the decoupling capacitor voltage u_b (decoupling inductor current i_L), decoupling capacitor current i_c (decoupling inductor voltage u_L), ripple power p_r, and the terminal voltage u_{ab} when the capacitor voltage (decoupling inductor current i_L) is controlled under different references. (a) $u_b(i_L)$ is controlled to be sine wave. (b) u_b is controlled to be higher than the terminal voltage. (c) u_b is controlled to be full-wave rectified sine wave. (d) u_b is controlled to be lower than the terminal voltage (i_L is controlled to be a sine waveform with a predetermined dc bias).

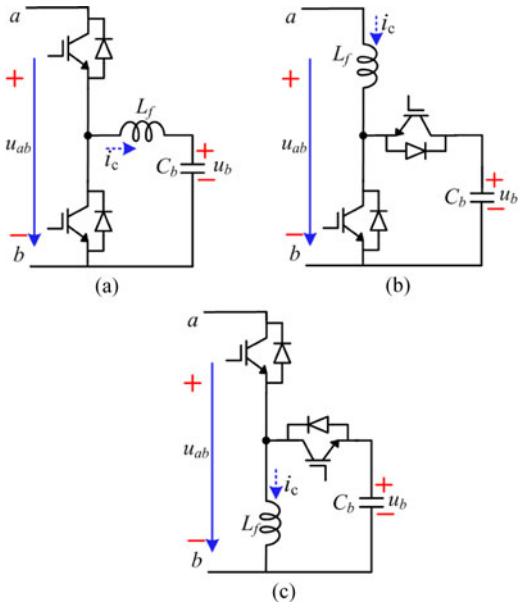

Fig. 4. Basic decoupling cell configured with bidirectional dc/dc circuits. (a) Buck-type basic decoupling cell. (b) Boost-type basic decoupling cell. (c) Buck–boost-type basic decoupling cell.

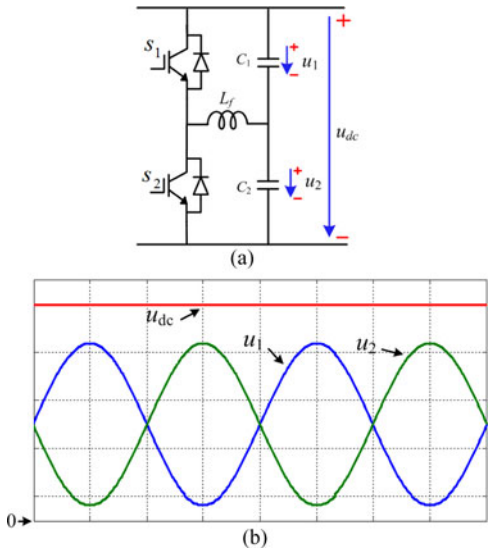

Fig. 5. Capacitor-split basic decoupling cell. (a) Schematic diagram. (b) Waveforms of the dc capacitors.

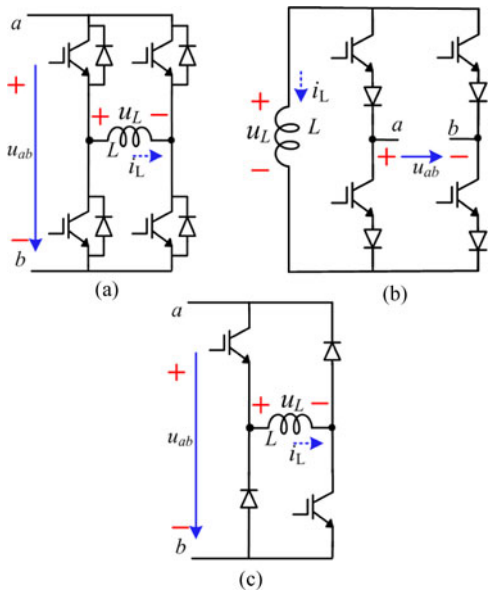

Fig. 6. H-bridge basic decoupling cell with an inductor as the energy storage unit. (a) With ac inductor current and dc terminal voltage. (b) With ac terminal voltage and dc inductor current. (c) With dc inductor current and terminal voltage.

boost-type basic decoupling cell as illustrated in Fig. 4(b). Such a simplification has no impact on the value of capacitance. In addition, it reduces cost and the system complexity. According to the characteristics of the basic cells in Fig. 4(a) and (b), it can be concluded that almost all the bidirectional dc/dc circuits are the candidates for the basic decoupling cells, for example, the bidirectional buck–boost circuit shown in Fig. 4(c). A merit of the buck–boost-type basic decoupling cell is that its capacitor voltage has no limitations and can be lower or higher than the terminal voltage u_{ab}, which widens the potential applications of the decoupling circuit. However, the drawbacks are the reduced efficiency and increased volume of the filter inductor L_f.

The ripple power, in all of the aforementioned basic decoupling cells, is buffered by a single capacitor. Fig. 5(a) shows a capacitor-split basic decoupling cell, in which the ripple power is buffered by two capacitors. Capacitors C_1 and C_2 are identical and connected in series. Usually, the capacitor voltage waveforms are regulated as shown in Fig. 5(b) by controlling the switches S_1 and S_2. The capacitors C_1 and C_2 play dual roles of mitigating the ripple power and filtering switching ripple.

2) Inductive Energy Storage: As well known, inductors can also be used as a kind of energy storage unit for electric energy, and superconducting magnetic energy storage is a classic example. For the basic decoupling cell based on the inductive energy storage, the ripple energy is stored in the electromagnetic field of inductors. Fig. 6(a) and (b) shows two basic decoupling cells with an inductor as the energy storage unit. The inductor in Fig. 6(a) is an ac inductor, and its current can be controlled to be a sine waveform without any dc bias, as shown in Fig. 3(a). However, the inductor current i_L in Fig. 6(b) is usually controlled to be a sine waveform with a predetermined dc bias to keep the unipolarity, as shown in Fig. 3(d). In Fig. 6(b) u_{ab} can be bipolar. However, in many occasions, it only needs to be connected to a dc voltage, and then its simplified version is obtained as shown in Fig. 6(c).

B. Current-Source-Oriented Basic Decoupling Cells

Regarding to basic decoupling cells applied to CSCs, usually a capacitor is selected as the ripple energy storage element, which guarantees the minimal order of the decoupling cells. According to the duality principle, two basic decoupling cells suited for the CSCs are derived from the basic cells in Fig. 6(a) and (b), which are illustrated in Fig. 7(a) and (b).

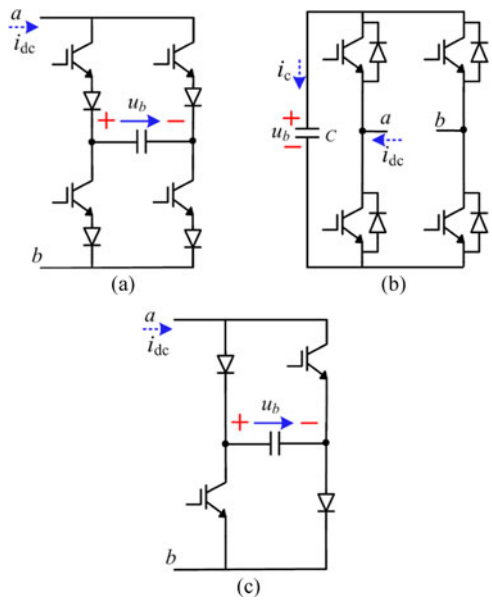

Fig. 7. Current-source-oriented basic decoupling cells. (a) With ac capacitor voltage and unidirectional terminal current. (b) With dc capacitor voltage and ac terminal current. (c) With dc capacitor voltage and terminal current.

The capacitor in Fig. 7(a) should withstand ac voltage but the terminal current $i_{\rm dc}$ is limited to be positive. The contrary is the case in Fig. 7(b). If the capacitor in Fig. 7(a) only needs to withstand a dc voltage or the terminal current $i_{\rm dc}$ of the cell in Fig. 7(b) is unidirectional, both of them can be simplified into the basic cell shown in Fig. 7(c).

IV. Independent Decoupling Topologies

Fig. 8 shows a broad categorization of the decoupling circuit topologies. The independent decoupling topologies discussed in this section mean the single-phase converters and the basic decoupling cells operate independently. Usually, the basic decoupling cell is connected to the dc link of the single-phase converters in parallel or series. The single-phase converter is responsible for regulating the dc-link voltage/current and basic decoupling cell's task is to deal with the ripple power. The introduction of the additional basic decoupling cell will not change the operation point of the original single-phase converter. Meanwhile, the control methods and modulation strategies for the original single-phase converter and the basic decoupling cell can be designed independently. In what follows, the independent decoupling circuit topologies will be reviewed.

Fig. 9 shows a single-phase VSC with the H-bridge basic decoupling cell in Fig. 2(a), where the basic decoupling cell is connected in parallel with the dc link [16], [17]. In [18], such a ripple decoupling concept is applied to unidirectional PFC rectifiers. In PV system with isolated transformer cases, the ripple decoupling concept above is well studied and further developed [19]. The capacitor voltage is preferred to be sine wave or full-wave rectified sine wave [16]–[20] for 100% voltage utilization ratio. Then, minimum capacitance requirements are achieved, which minimizes the cost and size of the energy storage capacitor.

Fig. 10 shows a framework of the general power conditioner with H-bridge basic decoupling cell in Fig. 2(b) in parallel and series. The basic idea of the parallel decoupling concept is to inject compensation current to the coupling point, which is able to prevent the twice current ripple from flowing into the dc capacitor [21], [22]. That idea is equivalent to the principle of the parallel active power filter. The basic idea of the series decoupling concept is to inject the compensation voltage in series to mitigate the pulsed voltage in dc-link voltage u_c caused by the twice ripple power [23]–[25], which is equivalent to the principle of the series active power filter. However, the series decoupling concept may be not very suitable for the applications in [23]–[25]. Although the dc-link voltage u_d fed to the right-side converter in Fig. 10(b) is smooth, the low-frequency ripple voltage in dc-link voltage u_c still exists. As a result, the effect of low-frequency ripple voltages on the MPPT efficiency of PV modules still needs to be taken into account [24].

The single-phase VSC with the buck-type basic decoupling cell as shown in Fig. 11 is first presented in [26]. The decoupling capacitor voltage u_b should be lower than the dc-link voltage u_c, which makes it suited for the cases where the dc-link voltage is relatively high. It has been further investigated in terms of operating principles, operation modes (DCM or CCM), and control strategies in a large number of literatures [27]–[33]. In this topology, the injected compensation current to dc link is discontinuous and the ripple energy is mainly stored in the capacitor C_b. To reduce the volume and weight of the decoupling cell, the inductance L_f is selected to be very small [27], [28]. In DCM, the buffered average power over each sampling period can be controlled accurately in open-loop control ways. In addition, it is possible to realize the zero-voltage switching. In CCM, to realize the power decoupling with an open-loop control, the reference of the voltage u_b should be calculated. However, according to [29], a complicated nonlinear differential equation needs to be solved. Only if the inductor L_f is so small that its effect can be neglected, the reference voltage can be easily solved. However, to make the inductor L_f small, a high switching frequency is needed, which in turn decreases the system efficiency. On the other hand, the peak current of the inductor L_f in DCM is much larger than that in CCM. Thus, semiconductor devices in DCM have to withstand higher current stress.

The single-phase VSC with a boost-type basic decoupling cell is illustrated in Fig. 12, which is a commonly used ripple power decoupling solution. Differing from the buck-type basic decoupling cell, the boost-type basic decoupling cell can inject continuous compensation current to the dc link. However, the decoupling capacitor voltage u_b must be regulated at a level higher than the dc-link voltage u_c, which makes it suited for the cases where the dc-link voltage is relatively low. A lot of researches on the boost-type basic decoupling cell have been carried out [34]–[46]. Lee *et al.* [34] investigated the component selection principle, and Palma *et al.* [35]–[40] mainly focused their attention on the control strategies. All the control strategies are open-loop control. To extract the reference for the current loop of the decoupling cell, simple low-pass filters [35] and resonant compensators [36] were applied. The low-pass filter

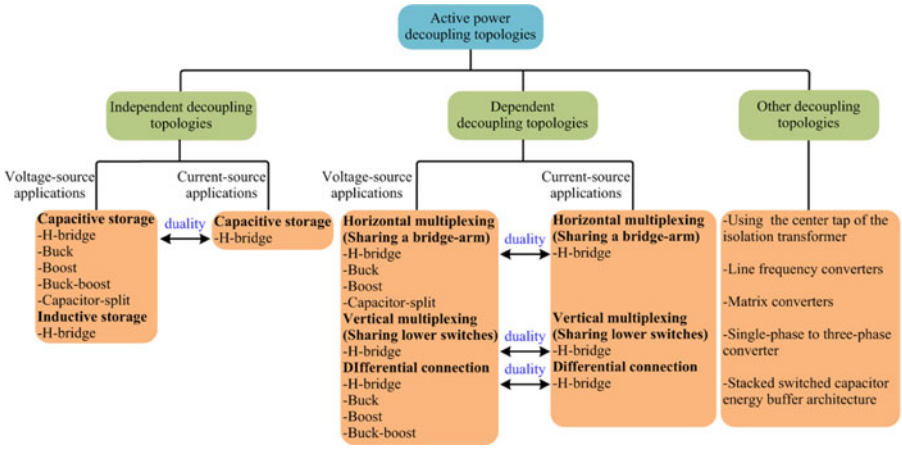

Fig. 8. Categorization of decoupling circuit topologies.

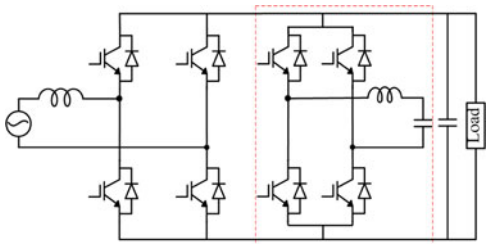

Fig. 9. Single-phase VSC with H-bridge basic decoupling cell in Fig. 2(a) [16]–[20].

is easy to implement but good control performance is hard to obtain. A low cutoff frequency means retarded response, while a high cutoff frequency means the extracted reference is not accurate enough. The resonant compensator in [36] is only designed to extract the twice ripple current; it has good dynamic response and steady-state performance. To design a current-loop controller of high performance, the repetitive control [36], multiresonant control [37], and feedforward control [38], [39] were proposed. The repetitive control could obtain good current steady-state tacking performance, but the computational burden is heavy. The multiresonant control is effective in this application and its computational burden decreases greatly compared to the repetitive control. The feedforward control based on the volt–second balance has the advantage of rapid dynamic response performance.

As well known, the aim of reducing capacitance and voltage stresses of the boost-type basic decoupling cell simultaneously is almost impossible. From a hardware perspective, the literature [41] presented a possible solution by recharging the decoupling capacitor via a small transformer and a diode rectifier from the grid. However, it causes distortions in the grid current. Another solution is to adopt the virtual capacitance control [42]. The main idea behind it is to change the dc-link voltage reference to stabilize the dc-link voltage.

In buck-type or boost-type basic decoupling cell, the decoupling capacitor voltage is limited to be lower or higher than the dc-link voltage. This limitation can be broken by using the

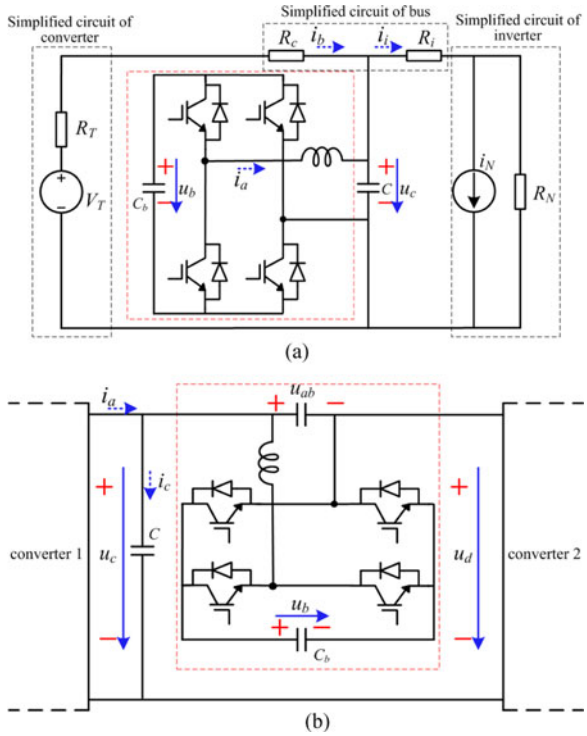

Fig. 10. Framework of general power conditioner with H-bridge basic decoupling cell in Fig. 2(b). (a) In parallel [21], [22]. (b) In series [23]–[25].

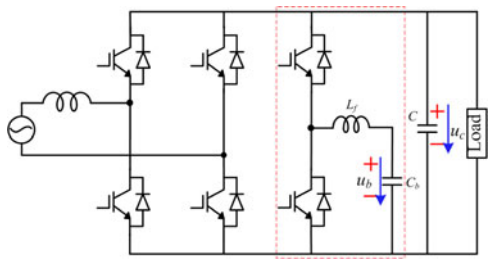

Fig. 11. Single-phase VSC with buck-type basic decoupling cell in Fig. 4(a) [26]–[33].

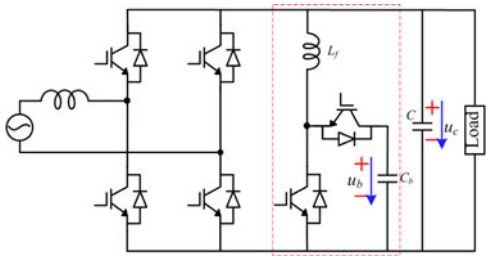

Fig. 12. Single-phase VSC with boost-type basic decoupling cell in Fig. 4(b) [34]–[46].

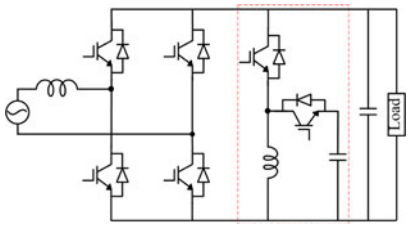

Fig. 13. Single-phase VSC with buck–boost-type basic decoupling cell in Fig. 4(c) [47].

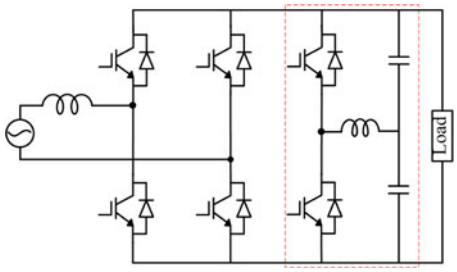

Fig. 14. Single-phase VSC with capacitor-split basic decoupling cell [48], [49], [78].

buck–boost-type basic decoupling cell as shown in Fig. 13. The decoupling concept was implemented under three different control methods in [47].

The single-phase converter with the capacitor-split basic decoupling cell is shown in Fig. 14. The capacitor-split basic decoupling cell is reported in [48] to reduce the high-frequency and the low-frequency current ripples in fuel cell. Accordingly, the stack efficiency and fuel utilization were significantly improved and the life of the fuel-cell stack was potentially enhanced. Thereafter, its decoupling appliances were investigated in [49] and [78]. The operation principle as well as an open-loop control was presented in [49]. To improve the system robustness and control performance, a closed-loop method was proposed in [78].

Most independent decoupling topologies use capacitors as the energy storage elements. Fig. 15 shows an independent decoupling topology in which the inductor is employed as the energy storage element. Compared with the aforementioned basic decoupling cells, it contains only one passive component. In [50], it is also called an active filter to replace the passive *LC* branch in traction vehicles to reduce the weight and save space. To

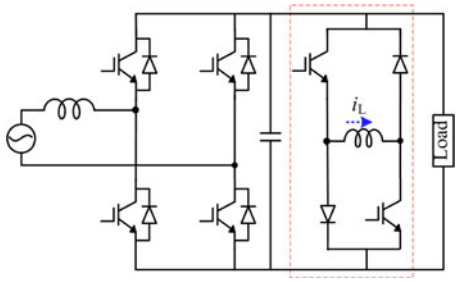

Fig. 15. Single-phase VSC with H-bridge basic decoupling cell in Fig. 6(c) [50].

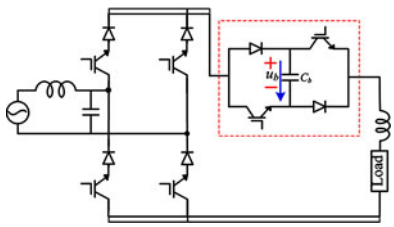

Fig. 16. Single-phase CSC with H-bridge basic decoupling cell in Fig. 7(c) [51].

avoid the discontinuous inductor current, the current reference for the decoupling inductor is a full-wave rectified sine wave with a certain offset.

All the independent decoupling topologies aforementioned are designed for the single-phase VSCs. Fig. 16 shows an independent decoupling topology tailored for CSCs. It is developed by connecting the H-bridge basic decoupling cell in Fig. 7(c) in series with the dc link [51]. It acts as a controlled voltage source to compensate the ripple component in the rectified output voltage, which is an example for the series decoupling concept. According to the duality principle, it is the dual topology of the converter shown in Fig. 9.

V. Dependent Decoupling Topologies

This section will review the dependent decoupling topologies in which the basic decoupling cell shares power semiconductor devices with the original converter partially and even fully. In the following section, the dependent decoupling topologies are also called "switch-multiplexing decoupling topologies."

A. Switch-Multiplexing Decoupling Topologies for Voltage-Source Applications

There are two different switch-multiplexing decoupling topologies derived from the converter shown in Fig. 9. The decoupling circuit with switch-multiplexing shown in Fig. 17(a) is proposed in [79]. The middle bridge-arm is shared by the original converter and the decoupling cell, which is termed as the horizontal multiplexing method. Then, the shared bridge-arm has to undertake two tasks simultaneously: rectification/inversion and ripple power buffering. One obvious advantage is that two active switches have been saved. However, there are also some weaknesses, for example, the viable operating range of the dc-link

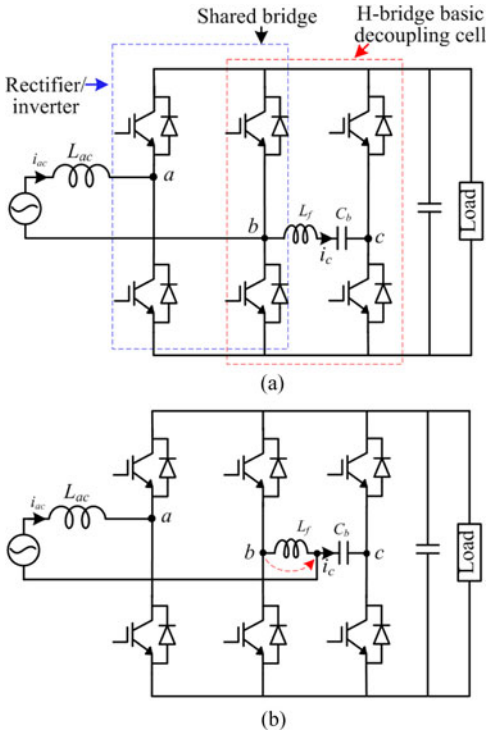

Fig. 17. Switch-multiplexing decoupling topology resulting from the topology in Fig. 9 (case one) [52], [53], [79]. (a) Main circuit. (b) Modified version.

voltage becomes smaller and the voltage stresses may become higher than those in the dependent decoupling topology. In [52] and [53], the switch-multiplexing decoupling circuit was also applied to single-phase reactive power compensation and the SVPWM was proposed to minimize voltage and current stress. Because the inductance L_f is so small that the voltage across it can be neglected, another decoupling circuit as shown in Fig. 17(b) can be obtained by a trivial modification. Clearly, the dynamics equations of the two converters shown in Fig. 17 are completely different. In Fig. 17(a), the input current is only determined by the voltage u_{ab}, and the decoupling current i_c is controlled by the voltage u_{bc}. If u_{ab} and u_{bc} meet the control requirements at any time, the dynamics of input current and decoupling current are decoupled. However, in Fig. 17(b), the input current dynamic is coupled with the voltage across the energy storage capacitor C_b, which complicates controller design.

Inspired by six switches single-phase ac/dc/ac converter [83] and/or nine switches three-phase ac/ac converter [84], another switch-multiplexing decoupling circuit is obtained as shown in Fig. 18. It is termed as the vertical multiplexing method. Differing from the horizontal multiplexing method, such kind of sharing does not affect the dc-link voltage utilization with a novel SVPWM [54].

Fig. 19(a) shows a switch-multiplexing decoupling circuit derived from the converter in Fig. 11. Because the voltage across the inductance L_f is small, another switch-multiplexing decoupling circuit [64] can be obtained by a trivial modification, which is illustrated in Fig. 19(b). Another switch-multiplexing decoupling circuit derived from the converter in Fig. 14 is shown in Fig. 20(a). It is first proposed in [65] and further investigated in [66] and [80]. For the same reason of small inductance L_f, another switch-multiplexing decoupling circuit shown in Fig. 20(b) could be obtained by changing a connection point [67]. Their difference lies in the control strategies. In [66] and [80], the ripple power is stored both in capacitors C_1 and C_2; while in [67], the ripple power is only stored in C_1 and the voltage across C_2 is controlled to be a constant. If the capacitor C_2 is replaced by a battery, the decoupling circuit shown in Fig. 20(c) will be obtained [68], [69]. Under such case, the twice ripple power is also buffered by C_1 only. The decoupling topologies in both Figs. 19 and 20 achieve switches minimization as no additional switches are added that reduces the cost to some extent. However, the decoupling topology in Fig. 20(a)

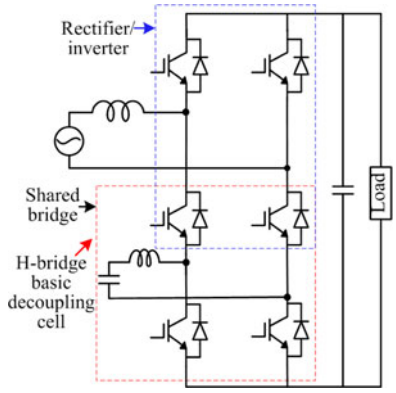

Fig. 18. Switch-multiplexing decoupling topology resulting from topology in Fig. 9 (case two) [54].

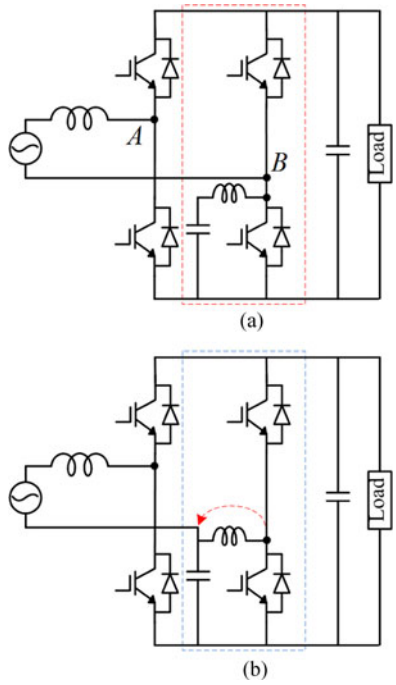

Fig. 19. Switch-multiplexing decoupling topology resulting from topology in Fig. 11. (a) Main circuit. (b) Modified version [64].

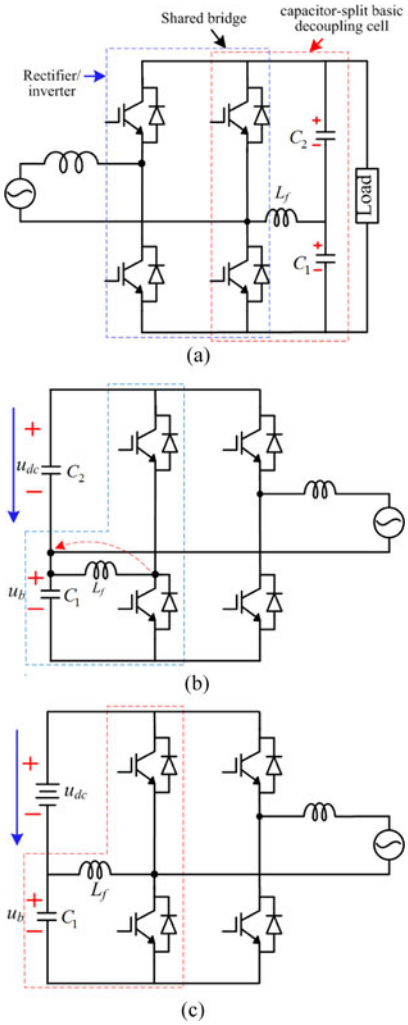

Fig. 20. Switch-multiplexing decoupling topologies resulting from topology in Fig. 14. (a) Main circuit [65], [66], [80]. (b) Modified version one [67]. (c) Modified version two [68], [69].

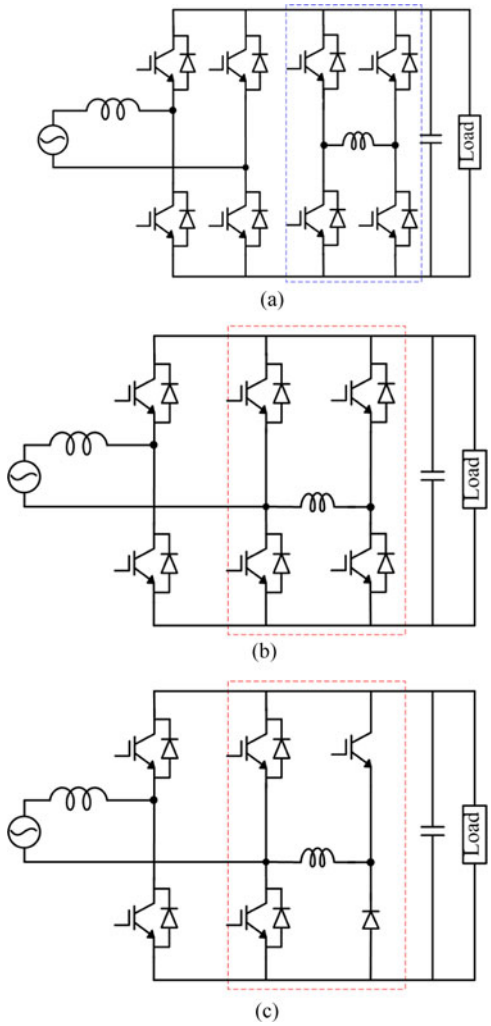

Fig. 21. Decoupling topologies resulting from H-bridge basic decoupling cell in Fig. 6(a). (a) Main circuit. (b) Switch-multiplexing decoupling circuit [55]–[59]. (c) Modified inversion [60].

is not recommended for inductive load because it will causes high current stress or voltage stress [78], and in (b) and (c), the switching devices suffer from high voltage stress $(u_{\rm dc} + u_b)$, which should be paid more attention when selecting suitable switches and doing thermal design.

Fig. 21(b) shows a switch-multiplexing decoupling circuit, which can be derived from the circuit shown in Fig. 21(a) by sharing one bridge-arm and is reported in [55]–[59]. The current through the energy storage inductor can be controlled to a sine waveform. If the current through the energy storage inductor is a dc current, some redundant switches can be removed, and the resulting decoupling circuit is shown Fig. 21(c) [60].

The aforementioned switch-multiplexing decoupling circuits are summarized from the point of the switching sharing concept. Besides, the differential connection is also an important way to construct decoupling circuit topologies. As well known, many classical ac/dc converters are derived from basic dc/dc converters by differential connection [85]. It is reported that dc/dc converters formed by differential connection have the inherent capability of ripple power decoupling by controlling the common-mode voltages of the output filter capacitors [70]–[76].

Fig. 22(a) shows a possible decoupling solution formed by two identical full-bridge inverters in differential connection way. As can be seen, it is obvious that the first or the fourth bridge-arm (from left to right) is redundant. After removing the redundant one, a simplified version shown in Fig. 22(b) is obtained [70], [71]. Through the analysis of circuit in Fig. 22(b), if the output terminal of the second bridge-arm is clamped to the negative busbar, the converter as shown in Fig. 22(c) [72], [73] is obtained. The main difference between converters in Fig. 22(b) and (c) is that the voltages across the C_1 and C_2 can be controlled to be ac voltages in the former, while only dc voltages in the latter. If the dc-link voltage, grid voltage, and decoupling capacitors in both of them are completely the same, the power decoupling capability of the former is more powerful than that of the latter. With regard to the decoupling topology in Fig. 22(c), actually, one of the decoupling capacitors can be removed. Then, the resulted circuit coincides with the converter

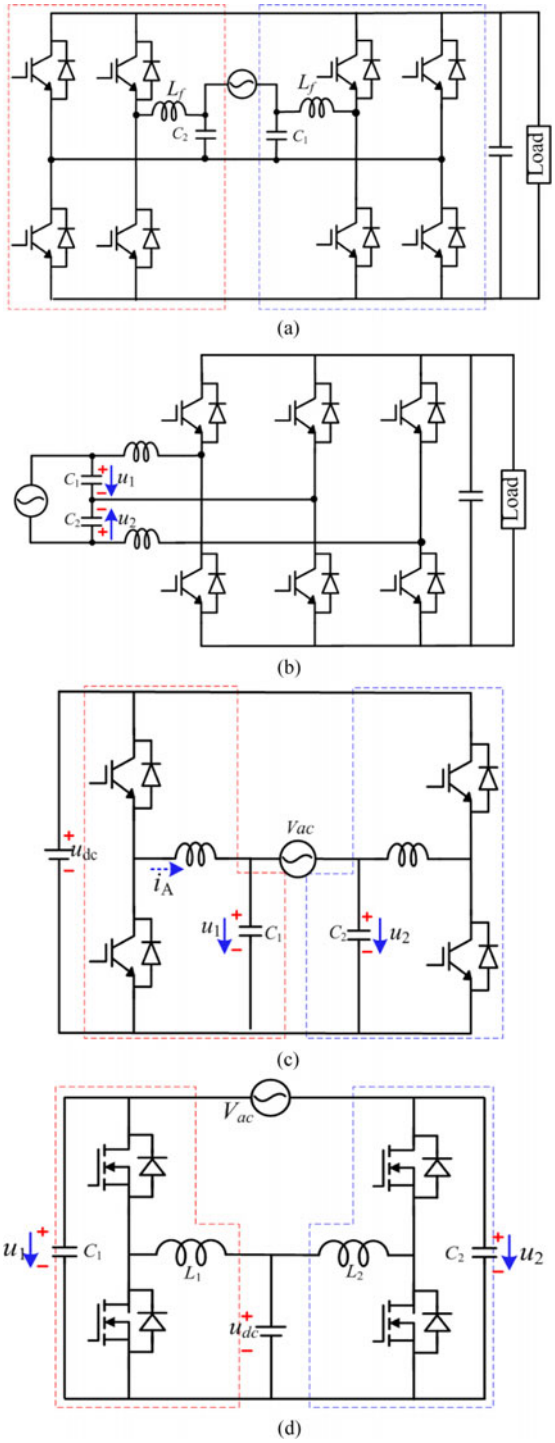

Fig. 22. Decoupling topologies with differential connection concept. (a) Two H-bridge basic decoupling cells in Fig. 2(a) connected in differential way. (b) Switch-multiplexing version resulting from (a) [70], [71]. (c) Buck-type differential inverter [72], [73]. (d) Boost-type differential inverter [74]–[76].

shown in Fig. 19(b). Besides the aforementioned buck-type differential inverters, there are other cases such as the boost-type concept shown in Fig. 22(d) and buck–boost-type concept [86]. Both of them could also achieve ripple power decoupling with proper control methods.

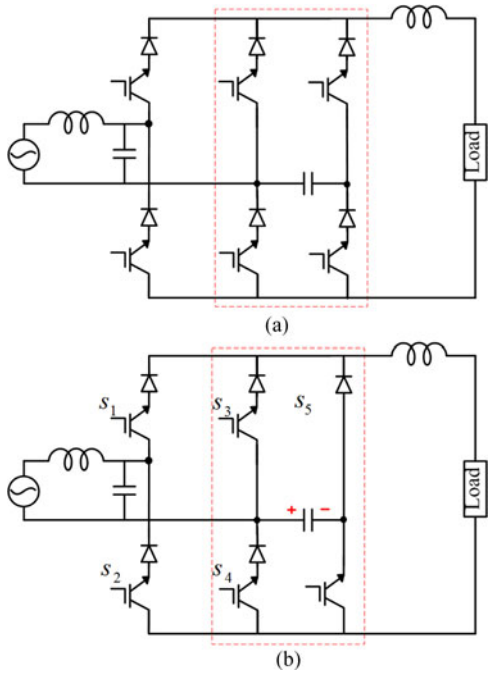

Fig. 23. Switch-multiplexing decoupling topologies resulting from H-bridge basic decoupling cell in Fig. 7(a) (case one) [59], [61], [62]. (a) Main circuit. (b) Modified inversion.

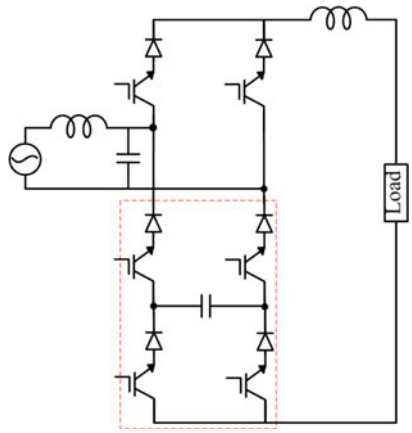

Fig. 24. Switch-multiplexing decoupling topology resulting from H-bridge basic decoupling cell in Fig. 7(a) (case two) [63].

B. Switch-Multiplexing Decoupling Topologies for Current-Source Applications

According to the duality principle, corresponding switch-multiplexing decoupling circuit topologies for CSCs could be derived from foregoing switch-multiplexing decoupling circuit topologies for VSCs.

Fig. 23(a) is a switch-multiplexing decoupling circuit formed by sharing one bridge-arm between the basic decoupling cell shown in Fig. 7(a) and a traditional current-source rectifier [59], [61], [62]. Meanwhile, it could also be viewed as the dual circuit of the converter shown in Fig. 21(b). If the energy storage capacitor in Fig. 23(a) only withstands the dc voltage, the converter

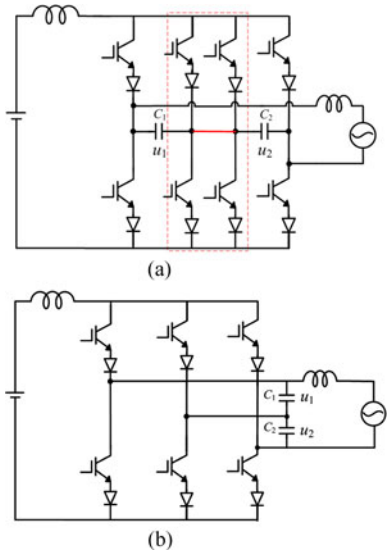

Fig. 25. Decoupling topologies with two H-bridge basic decoupling cells in Fig. 7(a) connected in differential way. (a) Main circuit. (b) Modified inversion [77].

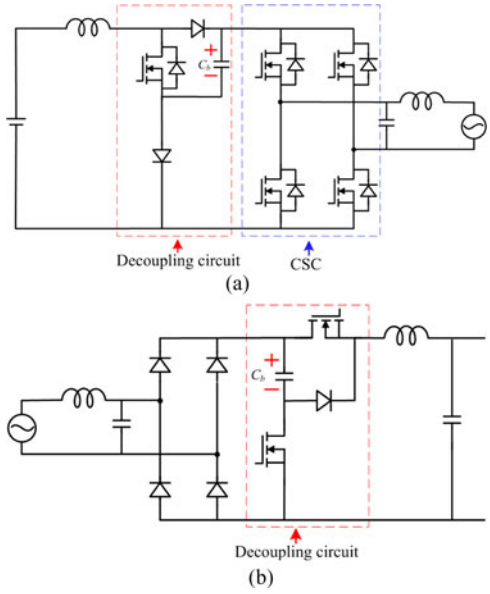

Fig. 27. Decoupling topologies in line frequency converters. (a) Inversion [81]. (b) Rectification [82].

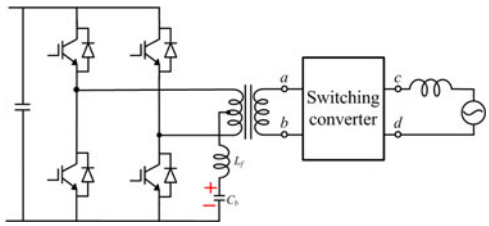

Fig. 26. Decoupling topology using the center tap of the isolation transformer [87], [88].

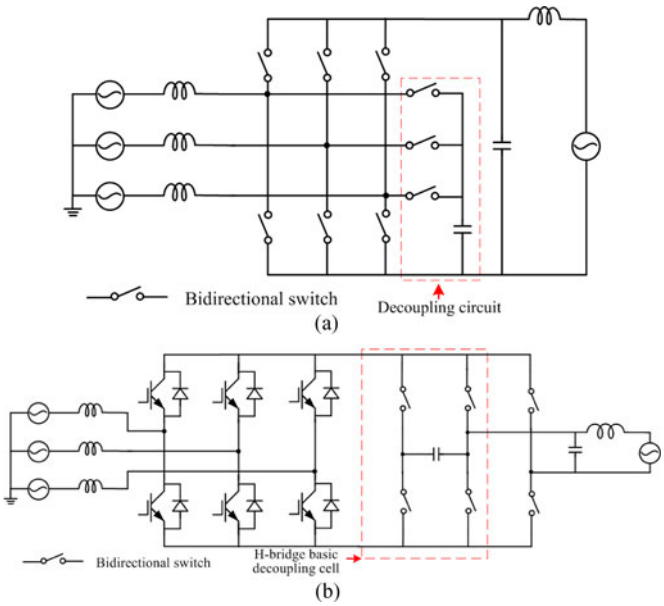

Fig. 28. Three-phase to single-phase matrix converter with an active power decoupling capacitor [89], [90]. (a) Main circuit. (b) Equivalent circuit.

shown in Fig. 23(b) can be obtained by removing redundant switches and diodes. Note that in Fig. 23(b), the decoupling capacitor voltage needs to be higher than the peak value of grid voltage when operating in inverting mode. However, the constraint is not needed in rectifying mode.

Fig. 24 shows a switch-multiplexing decoupling circuit formed by sharing two lower switches between the decoupling cell shown in Fig. 9(a) and a traditional current-source rectifier [63], which is slightly different from the decoupling topology shown in Fig. 23(a). In fact, it could be viewed as the dual circuit of the converter shown in Fig. 18.

The differential connection operation could also be applied to current-source inverters. Fig. 25(a) shows an inverter, which is formed by two identical current-source inverters connected in differential ways. Because the second or third bridge-arm (from left to right) is redundant, one of them can be removed. The resulted circuit [77] is shown in Fig. 25(b), which could be viewed as the dual circuit of the converter shown in Fig. 22(b). The voltages across the capacitors C_1 and C_2 are ac voltages, which results in low voltage stress.

VI. Other Active Decoupling Topologies

The special cases, which do not abide by the construction laws of decoupling circuits as clearly as those mentioned above, will be introduced in this section.

Fig. 26 shows a converter with the ripple power decoupling capability [87], [88]. Capacitor C_b is the energy storage unit, and a small inductor L_f is used for filtering. The common voltage is used to control the energy stored in capacitor C_b. The literature [81] proposed a single-phase dc–ac inverter with decoupling capability as shown in Fig. 27(a). The decoupling

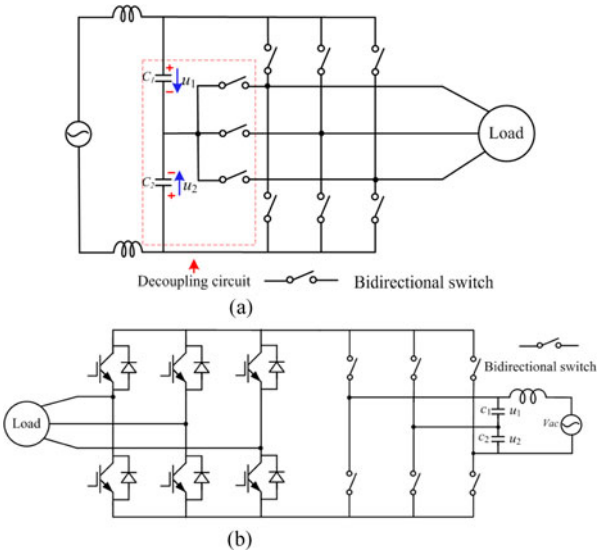

Fig. 29. Single-phase to three-phase matrix converter with differential connection decoupling concept [91]. (a) Main circuit. (b) Equivalent circuit.

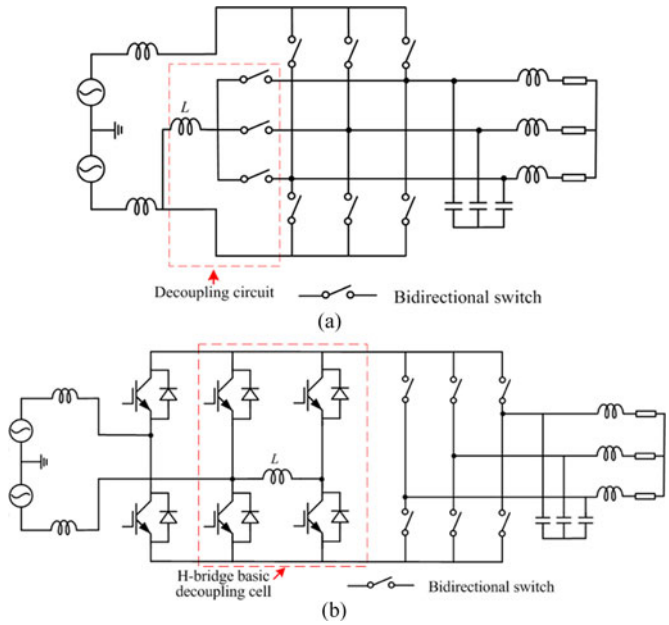

Fig. 30. Single-phase to three-phase matrix converter with an active power decoupling inductor [92]. (a) Main circuit. (b) Equivalent circuit.

cell only includes an energy storage capacitor C_b, one active switch, and two diodes. However, only the unilateral energy flow is permitted in this converter. A single-phase buck PFC ac–dc converter with the power decoupling capability is illustrated in Fig. 27(b) [82]. Compared with the conventional buck PFC ac–dc converter, only one additional energy storage capacitor and one MOSFET are needed. In Fig. 27, both of the decoupling capacitor voltages must be higher than the peak value of grid voltage for safety operation. Meanwhile, since the power factor control and the ripple power decoupling control are coupled to each other, the control is quite complicated.

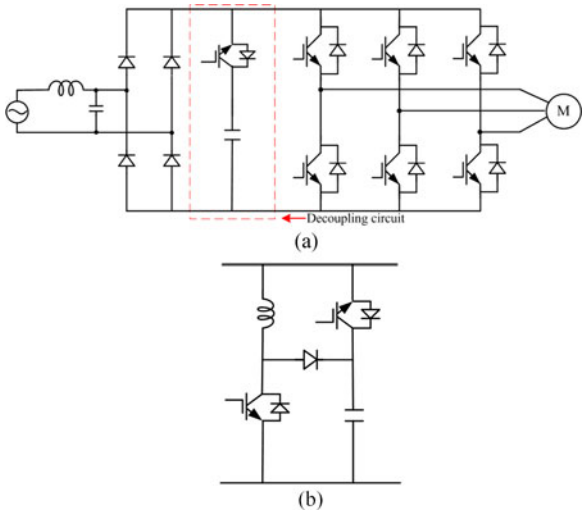

Fig. 31. Single-phase to three-phase converter with power decoupling function. (a) Main circuit [93]. (b) Improved buffer circuit [94].

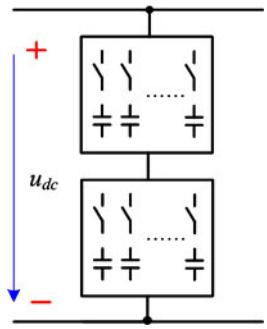

Fig. 32. SSC energy buffer architecture [96], [97].

Three-phase to three-phase matrix converters are studied comprehensively. However, in some applications, such as rail road system and home electronics equipments, single-phase to three-phase matrix converter is required. The same as single-phase rectifiers/inverters, the twice ripple power problem also exists in the single-phase to three-phase matrix converter. Three kinds of power decoupling methods have been developed [89]–[92]. The first power decoupling configuration is shown in Fig. 28(a), in which an energy storage capacitor is employed to buffer the ripple power. Its equivalent circuit is showed in Fig. 28(b), which is similar with the converter shown in Fig. 23(a). The second power decoupling configuration is shown in Fig. 29(a), in which the ripple power is stored in the split-capacitors. Its equivalent circuit is shown in Fig. 29(b), and its operation principle is similar with that of the converter in Fig. 25(b). The last decoupling configuration is shown in Fig. 30(a), where the ripple power is stored in the inductor L, and its equivalent circuit is shown in Fig. 30(b), which is similar with the converter shown in Fig. 21(b).

Ohnuma and Itoh [93] proposed a single-phase to three-phase converter with the power decoupling function as shown in Fig. 31(a). The leakage inductance of the induction machine fed by the inverter is used to transfer the energy between the

TABLE I
SUMMARY OF DECOUPLING TOPOLOGIES

Categorization	Decoupling technology	Power rating	Decoupling component (Value)	Adding cost	Efficiency(1)	Connection	Features	
Independent decoupling topologies	Fig. 9 [16]	200W	1 Capacitor (10uF)	4 Switches + 4 Diodes	-	In parallel, integrated through a winding	-Flexible control and modulation design	-Step-down voltage characteristic -Various decoupling capacitor voltage waveforms -A large number of switches
	Fig. 10 [22]	500W	1 Capacitor (-)	4 Switches + 4 Diodes	-	In parallel /series		-Flexible position -Step-up voltage characteristic -A large number of switches
	Fig. 11 [27]	1.5kW	1 Capacitor (200uF)	2 Switches + 2 Diodes	93.2%	In parallel		-Step-down voltage characteristic
	Fig. 12 [40]	2kW	1 Capacitor (100uF)	2 Switches + 2 Diodes	-	In parallel		-Step-up voltage characteristic
	Fig. 13 [47]	1kW	1 Capacitor (165uF)	2 Switches + 2 Diodes	-	In parallel		-Flexible capacitor voltage range
	Fig. 14 [49]	1kW	2 Capacitors (90uF each)	2 Switches + 2 Diodes	92.1%	In parallel		-Differential connection -Decoupling capacitors also works as output voltage filters
	Fig. 15 [50]	-	1 Inductor (2.5mH)	2 Switches + 2 Diodes	-	In parallel		-Flexible inductor current range
	Fig. 16 [51]	144W	1 Capacitor (91.8uF)	2 Switches + 2 Diodes	84%	In series		-Flexible capacitor voltage range
Dependent decoupling topologies	Fig. 17 [79]	4kW	1 Capacitor (220uF)	2 Switches + 2 Diodes	-	In parallel	-Cooperation with original converter -Increasing modulation and control complexity	-Partially reduced switches and diodes -Horizontal multiplexing -Viable operating range is limited and the voltage stress may become higher
	Fig. 18 [54]	1kW	1 Capacitor (132uF)	2 Switches + 2 Diodes	-	-		-Vertical multiplexing -Partially reduced switches and diodes -DC-link voltage regulation range is not affected
Dependent decoupling topologies	Fig. 19 [64]	7kW	1 Capacitor (700uF)	-	-	-	-Cooperation with original converter -Increasing modulation and control complexity	- No additional switches and diodes
	Fig. 20(b) [67]	181.8W	1 Capacitor (5uF)	-	-	-		-No additional switches and diodes -Switching voltage stresses are increased
	Fig. 20(c) [69]	500W	1 Capacitor (100uF)	-	93.2%	-		
	Fig. 21(b) [56]	600W	1 Inductor (28mH)	2 Switches + 2 Diodes	88%	In parallel		-Partially reduced switches and diodes -Horizontal multiplexing
	Fig. 21(c) [60]	192W	1 Inductor (10mH)	1 Switch+ 1 Diode	-	In parallel		
	Fig.23(a) [62]	1.5kW	1 Capacitor (300uF)	2 Switches + 2 Diodes	-	In parallel		-Partially reduced switches and diodes -Horizontal multiplexing
	Fig.24 [63]	1kW	1 Capacitor (50uF)	2 Switches + 2 Diodes	-	-		-Partially reduced switches and diodes -Vertical multiplexing
	Fig. 20(a) [80]	1kW	2 Capacitors (90uF each)	-	93.8%	Differential connection		-No additional switches and diodes -Decoupling capacitors also works as the output voltage/input filter -Distortion may be introduced into the utility current
	Fig. 22(c) [73]	1kW	2 Capacitors (60uF each)	-	90%			
	Fig. 22(d) [74]	170W	2 Capacitors (15uF each)	-	83%			
	Fig. 22(b) [70]	100W	2 Capacitors (165uF)	2 Switches + 2 Diodes	-			
	Fig. 25(b) [77]	1kW	2 Capacitors (32uF)	2 Switches + 2 Diodes	-			
Others	Fig. 26 [87]	1kW	1 Capacitor (440uF)	-	91%	Through the center tap	-No additional switches and diodes -DC-link voltage utilization ratio is impaired	
	Fig. 27(a) [81]	400W	1 Capacitor (50uF)	1 Mosfet+ 2 Diodes	94.9%	-	-Additional PFC function -Decoupling capacitor voltage must be higher than the peak value of grid voltage. -Increased modulation and control complexity	
	Fig. 27(b) [82]	750W	1 Capacitor (100uF)	2 Mosfets+ 1 Diode	96.4%	-		
	Fig. 28 [89]	400W	1 Capacitor (8.8uF)	3 Bidirectional switches	-	-	-Increased modulation and control complexity	
	Fig. 29 [91]	495W	2 Capacitors (15uF)	3 Bidirectional switches	-	-	-Increased modulation and control complexity -Decoupling capacitors also works as the input filter -Distortion may be introduced into the utility current	
	Fig. 30 [92]	3.7kW	1 Inductor (1mH)	3 Bidirectional switches	-	-	-Increased modulation and control complexity	
	Fig. 31(a) [93]	1kW	1 Capacitor (50uF)	1 Switch + 1 Diode	82.8%	In parallel	-Additional snubber function -Zero-current commutation -0.5 voltage transfer ratio	
	Fig. 31(b) [94]	1kW	1 Capacitor (100uF)	2 Switches + 2 Diodes	94.6%	In parallel	-Additional snubber function -Zero-current commutation -0.707 voltage transfer ratio	
	Fig. 32 [96]	135W	Multiple capacitors (2.2uF each)	Multiple switches +diodes	97%	In parallel	-Low (line-scale) switching frequencies -A very large number of switches and capacitors -requiring a precharge circuit	

(1) The efficiency comes from the given value or the efficiency curve in the corresponding references.

grid and energy storage capacitor. However, the voltage transfer ratio is less than 0.5. To improve the voltage transfer ratio, a circuit shown in Fig. 31(b) is used to replace the original decoupling circuit [94]. With the diodes in rectifier replaced by bidirectional switches, it becomes a single-phase to three-phase matrix converter with the power decoupling capability [95].

The stacked switched capacitor (SSC) energy buffer architecture is a new concept in ripple power decoupling techniques [96], [97]. It composes of two groups of switches and capacitors shown in Fig. 32. A method similar with the hysteresis control is used to determine the time at which a predefined switch combination is carried out. The ripple voltage can be limited in a small band. However, a perfect ripple decoupling is difficult to achieve, which is different from the decoupling methods mentioned above.

VII. Conclusion

Most of the active power decoupling topologies have been surveyed and categorized based on circuit properties and operation principle to provide researchers with a global picture of them. Table I summarizes the different active decoupling topologies predominant in the literature. Three concepts, i.e., "duality principle," "switches sharing," and "differential connection," have been used to explain and predict the evolution of the active power decoupling topologies.

According to the development path of the active power decoupling topologies, it seems that most researchers paid close attention to the topologies with low cost (reducing switches). For instance, the decoupling topologies from the early independent decoupling topologies with eight active switches to the latter multiplexing decoupling topologies with six active switches, five active switches, and even four active switches are proposed successively.

Active power decoupling topologies with the features of low cost, low volume and weight, high efficiency, high reliability, and high performance are always expected. However, there is no such thing as a free lunch. This may hold true for the active power decoupling methods. For independent decoupling topologies, decoupling circuits and original circuits are not interfered with each other, which lead to flexible designs in control methods and modulation strategies. However, this kind of decoupling method usually involves a lot of additional power semiconductor devices, which increases cost significantly. On the other hand, the power decoupling topologies with switch-multiplexing benefit from fewer power semiconductor devices. However, they usually suffer from more constraints, such as increasing voltage/current stress, reduced operation range, increased volume, and complicated control algorithms. Each active power decoupling topology has its advantages and disadvantages, so an evaluation method under multiobjective optimization framework should be studied to help to construct or select a proper topology for a specific application.

References

[1] B. Singh, B. N. Singh, A. Chandra, K. Al-Haddad, A. Pandey, and D. P. Kothari, "A review of single-phase improved power quality AC-DC converters," *IEEE Trans. Ind. Electron.*, vol. 50, no. 5, pp. 962–981, Oct. 2003.

[2] H. Hu, S. Harb, N. Kutkut, L. Batarseh, and Z. J. Shen, "A review of power decoupling techniques for microinverters with three different decoupling capacitor locations in PV systems," *IEEE Trans. Power Electron.*, vol. 28, no. 6, pp. 2711–2726, Jun, 2013.

[3] S. Li, S. C. Tan, C. Lee, E. Waffenschmidt, S. Y. R. Hui, and C. K. Tse, "A survey, classification and critical review of light-emitting diode drivers," *IEEE Trans. Power Electron.*, Mar. 2015, to be published.

[4] W. Chen and S. Y. R. Hui, "Elimination of an electrolytic capacitor in AC/DC light-emitting diode (LED) driver with high input power factor and constant output current," *IEEE Trans. Power Electron.*, vol. 27, no. 3, pp. 1598–1607, Mar. 2012.

[5] P. T. Krein and R. S. Balog, "Cost-effective hundred-year life for single phase inverters and rectifiers in solar and LED lighting applications based on minimum capacitance requirements and a ripple power port," in *Proc. IEEE Appl. Power Electron. Conf. Expo.*, Feb. 2009, pp. 620–625.

[6] H. Kim and K. Shin, "DESA: Dependable, efficient, scalable architecture for management of large-scale batteries," *IEEE Trans. Ind. Informat.*, vol. 8, no. 2, pp. 406–417, May 2012.

[7] F. Lacressonni, B. Cassoret, and J. F. Brudny, "Influence of a charging current with a sinusoidal perturbation on the performance of a lead–acid battery," *Proc. Inst. Elect. Eng., Elect. Power Appl.*, vol. 152, no. 5, pp. 1365–1370, Sep. 2005.

[8] G. Fontes, C. Turpin, S. Astier, and T. A. Meynard, "Interactions between fuel cells and power converters: Influence of current harmonics on a fuel cell stack," *IEEE Trans. Power Electron*, vol. 22, no. 2, pp. 670–678, Mar. 2007.

[9] R. S. Gemmen, "Analysis for the effect of inverter ripple current on fuel cell operating condition," *J. Fluids Eng.*, vol. 125, no. 3, pp. 576–585, May 2003.

[10] P. Dahler, G. Knapp, and A. Nold, "New generation of compact low voltage IGBT converter for traction applications," in *Proc. IEEE Eur. Conf. Power Electron. Appl.*, 2005, pp. 9–18.

[11] S. Nonaka and Y. Neba, "Single-phase PWM current source converter with double-frequency parallel resonance circuit for DC smoothing," in *Proc. Conf. Rec. IEEE-IAS Annu. Meet.*, 1993, pp. 1144–1151.

[12] M. Vasiladiotis and A. Rufer, "Dynamic analysis and state feedback voltage control of single-phase active rectifiers with DC-link resonant filters," *IEEE Trans. Power Electron*, vol. 29, no. 10, pp. 5620–5633, Oct. 2014.

[13] W. Huai, M. Liserre, and F. Blaabjerg, "Toward reliable power electronics: Challenges, design tools, and opportunities," *IEEE Ind. Electron. Mag.*, vol. 7, no. 2, pp. 17–26, Jun. 2013.

[14] H. Wang and F. Blaabjerg, "Reliability of capacitors for DC-link applications in power electronic converters—An overview," *IEEE Trans. Ind. Appl.*, vol. 50, no. 5, pp. 3569–3578, Sep./Oct. 2014.

[15] S. Dusmez and A. Khaligh, "Generalized technique of compensating low-frequency component of load current with a parallel bidirectional DC/DC converter," *IEEE Trans. Power Electron.*, vol. 29, no. 11, pp. 5892–5904, Nov. 2014.

[16] P. T. Krein, R. S. Balog, and M. Mirjafari, "Minimum energy and capacitance requirements for single-phase inverters and rectifiers using a ripple port," *IEEE Trans. Power Electron.*, vol. 27, no. 11, pp. 4690–4698, Nov. 2012.

[17] P. T. Krein and R. S. Balog, "Cost-effective hundred-year life for single-phase inverters and rectifiers in solar and LED lighting applications based on minimum capacitance requirements and a ripple power port," in *Proc. IEEE Appl. Power Electron. Conf.*, Washington, DC, USA, 2009, pp. 620–625.

[18] B. Tian, S. Harb, and R. S. Balog, "Ripple-port integrated PFC rectifier with fast dynamic response," in *Proc. IEEE Midwest Symp. Circuits Syst.*, College Station, TX, USA, 2014, pp. 781–784.

[19] S. Harb, M. Mirjafari, and R. S. Balog, "Ripple-port module-integrated inverter for grid-connected PV applications," *IEEE Trans. Ind. Appl.*, vol. 49, no. 6, pp. 2692–2698, Nov./Dec. 2013.

[20] S. Harb and R. S. Balog, "Single-phase PWM rectifier with power decoupling ripple-port for double-line-frequency ripple cancellation," in *Proc. IEEE Appl. Power Electron. Conf.*, Long Beach, CA, USA, 2013, pp. 1025–1029.

[21] X. Ma, B. Wang, F. Zhao, G. Qu, D. Gao, and Z Zhou, "A high power low ripple high dynamic performance DC power supply based on thyristor converter and active filter," in *Proc. IEEE 28th Annu. Conf. Ind. Electron. Soc.*, 2002, pp. 1238–1242.

[22] R. J. Wai and C. Y. Lin, "Active low-frequency ripple control for clean-energy power-conditioning mechanism," *IEEE Trans. Ind. Electron.*, vol. 57, no. 11, pp. 3780–3792, Nov. 2010.

[23] H. Wang, H. S. H. Chung, and W. Liu, "Use of a series voltage compensator for reduction of the DC-link capacitance in a capacitor-supported system," *IEEE Trans. Power Electron.*, vol. 29, no. 3, pp. 1163–1175, Mar. 2014.

[24] W. Liu, K. Wang, H. Chung, and S. Chuang, "Modeling and design of series voltage compensator for reduction of DC link capacitance in grid-tie solar inverter," *IEEE Trans. Power Electron.*, vol. 30, no. 5, pp. 2534–2548, May 2015.

[25] H. Wang, W. Liu, H. Chung, and F. Blaabjerg, "Stability analysis and dynamic response of a DC-link module with a series voltage compensator," in *Proc. IEEE Energy Convers. Congr. Expo.*, Denver, CO, USA, 2013, pp. 2453–2460.

[26] M. Saito and N. Matsui, "Modeling and control strategy for a single-phase PWM rectifier using a single-phase instantaneous active/reactive power theory," in *Proc. 25th Int. Telecommun. Energy Conf.*, 2003, pp. 573–578.

[27] R. Wang, F. Wang, D. Boroyevich, R. Burgos, R. Lai, P. Ning, and K. Rajashekara, "A high power density single-phase PWM rectifier with active ripple energy storage," *IEEE Trans. Power Electron.*, vol. 26, no. 5, pp. 1430–1443, May 2011.

[28] R. Wang, F. Wang, D. Boroyevich, and P. Ning, "A high power density single phase PWM rectifier with active ripple energy storage," in *Proc. IEEE Appl. Power Electron. Conf.*, Palm Springs, CA, USA, 2010, pp. 1378–1383.

[29] H. Li, K. Zhang, and H. Zhao, "DC-link active power filter for high-power single-phase PWM converters," *J. Power Electron.*, vol. 12, no. 3, pp. 458–467, May 2012.

[30] H. Li, K. Zhang, and H. Zhao, "Active DC-link power filter for single phase PWM rectifiers," in *Proc. IEEE Int. Conf. Power Electron. ECCE Asia*, Jeju, South Korea, 2011, pp. 2920–2926.

[31] C. Y. Wu, C. H. Chen, J. W. Cao, and M. T. Liu, "Power control and pulsation decoupling in a single-phase grid-connected voltage-source inverter," in *Proc. IEEE TENCON Spring Conf.*, Sydney, N.S.W., Australia, 2013, pp. 475–479.

[32] M. Jang, M. Ciobotaru, and V. G. Agelidis, "A single-stage fuel cell energy system based on a buck–boost inverter with a backup energy storage unit," *IEEE Trans. Power Electron.*, vol. 27, no. 6, pp. 2825–2834, Jun. 2012.

[33] M. Jang and V. G. Agelidis, "A minimum power-processing-stage fuel-cell energy system based on a boost-inverter with a bidirectional backup battery storage," *IEEE Trans. Power Electron.*, vol. 26, no. 5, pp. 1568–1577, May 2011.

[34] S. Y. Lee, Y. L. Chen, Y. M. Chen, and K. H. Liu, "Development of the active capacitor for PFC converters," in *Proc. IEEE Energy Convers. Congr. Expo.*, Pittsburgh, PA, USA, 2014, pp. 1522–1527.

[35] L. Palma, "An active power filter for low frequency ripple current reduction in fuel cell applications," in *Proc. IEEE Int. Symp. Power Electron. Elect. Drives Autom. Motion*, Pisa, Italy, 2010, pp. 1308–1313.

[36] Q. C. Zhong, W. L. Ming, X. Cao, and M. Krstic, "Reduction of DC-bus voltage ripples and capacitors for single-phase PWM-controlled rectifiers," in *Proc. IEEE Annu. Conf. Ind. Electron. Soc.*, Montreal, QC, Canada, 2012, pp. 1308–1313.

[37] I. Serban and C. Marinescu, "Active power decoupling circuit for a single-phase battery energy storage system dedicated to autonomous microgrids," in *Proc. IEEE Int. Symp. Ind. Electron.*, Bari, Italy, 2010, pp. 2717–2722.

[38] Y. Yang, X. Ruan, L. Zhang, J. He, and Z. Ye, "Feed-forward scheme for an electrolytic capacitor-less AC/DC LED driver to reduce output current ripple," *IEEE Trans. Power Electron.*, vol. 29, no. 10, pp. 5508–5517, Jun. 2014.

[39] S. Wang, X. Ruan, K. Yao, S. Tan, Y. Yang, and Z. Ye, "A flicker-free electrolytic capacitor-less AC–DC LED driver," *IEEE Trans. Power Electron.*, vol. 27, no. 11, pp. 4540–4548, Nov. 2012.

[40] W. Cai, B. Liu, S. Duan, and L. Jiang, "An active low-frequency ripple control method based on the virtual capacitor concept for BIPV systems," *IEEE Trans. Power Electron.*, vol. 29, no. 4, pp. 1733–1745, Apr. 2014.

[41] A. C. Kyritsis, N. P. Papanikolaou, and E. C. Tatakis, "Enhanced current pulsation smoothing parallel active filter for single stage grid-connected AC-PV modules," in *Proc. IEEE Power Electron. Motion Control Conf.*, Poznan, Poland, 2008, pp. 1287–1292.

[42] F. Schimpf and L. Norum, "Effective use of film capacitors in single-phase PV-inverters by active power decoupling," in *Proc. IEEE Annu. Conf. Ind. Electron. Soc.*, Glendale, AZ, USA, 2010, pp. 2784–2789.

[43] H. Shin and J. I. Ha, "Active DC-link circuit for single-phase diode rectifier system with small capacitance," in *Proc. IEEE Int. Electron. Appl. Conf. Expo.*, Shanghai, China, 2014, pp. 875–880.

[44] Y. Tang, D. Zhu, C. Jin, P. Wang, and F. Blaabjerg, "A three-level quasi-two-stage single-phase PFC converter with flexible output voltage and improved conversion efficiency," *IEEE Trans. Power Electron.*, vol. 30, no. 2, pp. 717–726, Feb. 2015.

[45] A. C. Kyritsis, N. P. Papanikolaou, and E. C. Tatakis, "A novel parallel active filter for current pulsation smoothing on single stage grid-connected AC-PV modules," in *Proc. IEEE Power Electron. Appl.*, Aalborg, Denmark, 2007, pp. 1–10.

[46] C. T. Lee, Y. M. Chen, L. C. Chen, and P. T. Cheng, "Efficiency improvement of a DC/AC converter with the power decoupling capability," in *Proc. IEEE Appl. Power Electron. Conf.*, Orlando, FL, USA, 2012, pp. 1462–1468.

[47] X. Cao, Q. Zhong, and W. Ming, "Ripple eliminator to smooth DC-Bus voltage and reduce the total capacitance required," *IEEE Trans. Power Electron.*, vol. 62, no. 4, pp. 2224–2235, Apr. 2015.

[48] S. K. Mazumder, R. K. Burra, and K. Acharya, "A ripple-mitigating and energy-efficient fuel cell power-conditioning system," *IEEE Trans. Power Electron.*, vol. 22, no. 4, pp. 1437–1452, Jul. 2007.

[49] Y. Tang, F. Blaabjerg, P. C. Loh, C. Jin, and P. Wang, "Decoupling of fluctuating power in single-phase systems through a symmetrical half-bridge circuit," *IEEE Trans. Power Electron.*, vol. 30, no. 4, pp. 1855–1865, Apr. 2015.

[50] T. Larsson and S. Ostlund, "Active DC link filter for two frequency electric locomotives," in *Proc. Electr. Railways United Eur. Conf.*, Amsterdam, the Netherlands, 1995, pp. 97–100.

[51] H. Han, Y. Liu, Y. Sun, M. Su, and W. Xiong, "Single-phase current source converter with power decoupling capability using a series-connected active buffer," *IET Power Electron.*, vol. 8, no. 5, pp. 700–707, May 2015.

[52] R. Chen, Y. Liu, and F. Z. Peng, "DC capacitor-less inverter for single-phase power conversion with minimum voltage and current stress," *IEEE Trans. Power Electron.*, vol. 30, no. 10, pp. 5499–5507, Oct. 2015.

[53] S. Liang, X. Lu, R. Chen, Y. Liu, S. Zhang, and F. Z. Peng, "A solid state variable capacitor with minimum DC capacitance," in *Proc. IEEE Appl. Power Electron. Conf.*, Fort Worth, TX, USA, 2014, pp. 3496–3501.

[54] S. Fan, Y. Xue, and K. Zhang, "Novel active power decoupling method for single-phase photovoltaic or energy storage applications," in *Proc. IEEE Energy Convers. Congr. Expo.*, Raleigh, NC, USA, 2012, pp. 2439–2446.

[55] T. Shimizu, Y. Fujioka, and G. Kimura, "DC ripple current reduction method on a single phase PWM voltage source converter," in *Proc. IEEE Power Conver. Conf.*, Nagaoka, Japan, 1997, pp. 237–240.

[56] T. Shimizu, Y. Jin, and G. Kimura, "DC ripple current reduction on a single-phase PWM voltage-source rectifier," *IEEE Trans. Ind. Appl.*, vol. 36, no. 4, pp. 1419–1429, Sep./Oct. 2000.

[57] C. Zonxiang, L. Chao, Y. Fenghua, and G. LiuSheng, "A single-phase grid-connected inverter with an active power decoupling circuit," in *Proc. IEEE Chin. Control Decis. Conf.*, Taiyuan, China, 2012, pp. 2806–2810.

[58] K. Tsuno, T. Shimizu, K. Wada, and K. Ishii, "Optimization of the DC ripple energy compensating circuit on a single-phase voltage source PWM rectifier," in *Proc. IEEE 35th Annu. Power Electron. Spec. Conf.*, 2004, vol. 1, pp. 316–321.

[59] M. A. Vitorino and M. B. D. R. Correa, "Compensation of DC link oscillation in single-phase VSI and CSI converters for photovoltaic grid connection," *IEEE Trans. Ind. Appl.*, vol. 50, no. 3, pp. 2021–2028, May/Jun. 2014.

[60] M. Su, P. Pan, X. Long, Y. Sun, and J. Yang, "An active power-decoupling method for single-phase AC-DC converters," *IEEE Trans. Ind. Informat.*, vol. 10, no. 1, pp. 461–468, Feb. 2014.

[61] C. R. Bush and B. Wang, "A single-phase current source solar inverter with reduced-size DC link," in *Proc. IEEE Energy Convers. Congr. Expo.*, San Jose, CA, USA, 2009, pp. 54–59.

[62] M. Saisho, T. Harimoto, H. Hayashi, and M. Saito, "Development of single-phase current source inverter with power decoupling function," in *Proc. IEEE Int. Conf. Power Electron. Drive Syst.*, Kitakyushu, Japan, 2013, pp. 591–596.

[63] M. A. Vitorino, L. V. Hartmann, D. A. Fernandes, L. E. Silva, and M. B. R. Correa, "Single-phase current source converter with new modulation approach and power decoupling," in *Proc. IEEE Appl. Power Electron. Conf.*, Fort Worth, TX, USA, 2014, vol. 3, pp. 2200–2207.

[64] W. Qi, H. Wang, X. Tan, G. Wang, and K. D. T. Ngo, "A novel active power decoupling single-phase PWM rectifier topology," in *Proc. IEEE Appl. Power Electron. Conf.*, Fort Worth, TX, USA, 2014, vol. 3, pp. 89–95.

[65] H. Zhao, H. Lin, C. Min, and K. Zhang, "A modified single-phase H-bridge PWM rectifier with power decoupling," in *Proc. IEEE Annu. Conf. Ind. Electron. Soc.*, Montreal, QC, Canada, 2012, pp. 80–85.

[66] A. K. Verma, B. Singh, and D. T. Shahani, "Electric vehicle and grid interface with modified PWM rectifier and DC-DC converter with power decoupling and unity power factor," in *Proc. IEEE India Int. Conf. Power Electron.*, Delhi, India, 2012, pp. 1–6.
[67] W. Ming, Q. Zhong, and X. Zhang, "Transformerless single-phase rectifiers with significantly reduced capacitance," *IEEE Trans. Power Electron.*, 2015, to be published.
[68] W. Cai, L. Jiang, B. Liu, and C. Zou, "A power decoupling method based on four-switch three-port DC/DC/AC converter in DC microgrid," in *Proc. IEEE Energy Convers. Congr. Expo.*, Denver, CO, USA, 2013, pp. 4678–4682.
[69] W. Cai, L. Jiang, B. Liu, and C. Zou, "A power decoupling method based on four-switch three-port DC/DC/AC converter in dc microgrid," *IEEE Trans. Ind. Appl.*, vol. 51, no. 1, pp. 336–343, Jan./Feb. 2015.
[70] T. Shimizu, T. Fujita, G. Kimura, and J. Hirose, "A unity power factor PWM rectifier with DC ripple compensation," *IEEE Trans. Ind. Electron.*, vol. 44, no. 4, pp. 447–455, Aug. 1997.
[71] T. Shimizu, T. Fujita, G. Kimura, and J. Hirose, "Unity-power-factor PWM rectifier with DC ripple compensation," in *Proc. IEEE Int. Conf. Ind. Electron. Control Instrum.*, Bologna, Italy, 1994, pp. 657–662.
[72] I. Serban, "A novel transistor-less power decoupling solution for single-phase inverters," in *Proc. IEEE Annu. Conf. Ind. Electron. Soc.*, Vienna, Austria, 2013, pp. 1496–1500.
[73] I. Serban, "Power decoupling method for single-phase h-bridge inverters with no additional power electronics," *IEEE Trans. Ind. Electron.*, vol. 62, no. 8, pp. 4805–4813, Aug. 2015.
[74] G. R. Zhu, S. C. Tan, Y. Chen, and C. K. Tse, "Mitigation of low-frequency current ripple in fuel-cell inverter systems through waveform control," *IEEE Trans. Power Electron.*, vol. 28, no. 2, pp. 779–792, Feb. 2013.
[75] S. Li, G. R. Zhu, S. C. Tan, and S. Y. Hui, "Direct AC/DC rectifier with mitigated low-frequency ripple through inductor-current waveform control," *IEEE Trans. Power. Electron.*, vol. 30, no. 8, pp. 4336–4348, Aug. 2015.
[76] S. Li, G. Zhu, S. C. Tan, and S. Y. Hui, "Direct AC/DC rectifier with mitigated low-frequency ripple through waveform control," in *Proc. IEEE Energy Convers. Congr. Expo.*, Pittsburgh, PA, USA, 2014, pp. 2691–2697.
[77] M. A. Vitorino, M. B. R. Correa, and C. B. Jacobina, "Single-phase power compensation in a current source converter," in *Proc IEEE Energy Convers. Congr. Expo.*, Denver, CO, USA, 2013, pp. 5288–5293.
[78] Y. Tang, Z. Qin, F. Blaabjerg, and P. C. Loh, "A dual voltage control strategy for single-phase PWM converters with power decoupling function," *IEEE Trans. Power Electron.*, vol. 30, no. 12, pp. 7060–7071, Dec. 2015.
[79] H. Li, K. Zhang, H. Zhao, S. Fan, and J. Xiong, "Active power decoupling for high-power single-phase PWM rectifiers," *IEEE Trans. Power Electron.*, vol. 28, no. 3, pp. 1308–1319, Mar. 2013.
[80] Y. Tang and F. Blaabjerg, "A component-minimized single-phase active power decoupling circuit with reduced current stress to semiconductor switches," *IEEE Trans. Power Electron.*, vol. 30, no. 6, pp. 2905–2910, Jun. 2015.
[81] Y. Ohnuma, K. Orikawa, and J. I. Itoh, "A single-phase current-source PV inverter with power decoupling capability using an active buffer," *IEEE Trans. Ind. Appl.*, vol. 51, no. 1, pp. 531–538, Jan./Feb. 2015.
[82] Y. Ohnuma and J. I. Itoh, "A novel single-phase buck PFC ac–dc converter with power decoupling capability using an active buffer," *IEEE Trans. Ind. Appl.*, vol. 50, no. 3, pp. 1905–1914, May/Jun. 2014.
[83] X. Liu, P. Wang, P. C. Loh, F. Blaabjerg, and X. Mingyu, "Six switches solution for single-phase AC/DC/AC converter with capability of second-order power mitigation in DC-link capacitor," in *Proc. IEEE Energy Convers. Congr. Expo.*, Phoenix, AZ, USA, 2011, pp. 1368–1375.
[84] C. Liu, B. Wu, N. R. Zargari, D. Xu, and J. Wang, "A novel three-phase three-leg ac/ac converter using nine IGBTs," *IEEE Trans. Power Electron*, vol. 24, no. 5, pp. 1151–1160, May 2009.
[85] R. W. Erickson and D. Maksimovic, "Converter circuits," in *Fundamentals Power Electronics*, 2nd ed. New York, NY, USA: Springer-Verlag, 2001, pp. 131–176.
[86] J. Almazan, N. Vazquez, and C. Hernandez, "A comparison between the buck, boost and buck-boost inverters," in *Proc. IEEE Int. Power Electron. Congr.*, Acapulco, Mexico, 2000, pp. 341–346.
[87] J. I. Itoh and F. Fayashi, "Ripple current reduction of a fuel cell for a single-phase isolated converter using a dc active filter with a center tap," *IEEE Trans. Power Electron.*, vol. 25, no. 3, pp. 550–556, Mar. 2010.
[88] H. Takahashi, N. Takaoka, R. R. R. Gutierrez, and J.-I. Itoh, "Power decoupling method for isolated dc to single-phase ac converter using matrix converter," in *Proc. IEEE Int. Conf. Ind. Electron. Soc.*, Dallas, TX, USA, 2014, pp. 3337–3343.
[89] H. Wu, H. Ge, Y. Xu, and W. Zhang, "The power factor correction of three-phase to single-phase matrix converter with an active power decoupling capacity," in *Proc. IEEE Conf. Expo. Transp. Electrification Asia-Pacific*, Beijing, China, 2014, pp. 1–5.
[90] Y. Miura, T. Amano, and T. Ise, "Hybrid control scheme of power compensation and modulation for a three-phase to single-phase matrix converter with a small capacitor," in *Proc. IEEE Int. Power Electron. Conf.*, Sapporo, Japan, 2010, pp. 1780–1787.
[91] Y. Furuhashi and T. Takeshita, "Single-phase to three-phase matrix converter with compensation for instantaneous-power fluctuation," in *Proc. IEEE 37th Annu. Conf. Ind. Electron. Soc.*, Melbourne, Vic., Auatralia, 2011, pp. 1572–1577.
[92] M. Saito, T. Takeshita, and N. Matsui, "A single to three phase matrix converter with a power decoupling capability," in *Proc. IEEE Power Electron. Spec. Conf.*, 2004, pp. 2400–2405.
[93] Y. Ohnuma and J. I. Itoh, "Space vector modulation for a single phase to three phase converter using an active buffer," in *Proc. IEEE Int. Power Electron. Conf.*, Sapporo, Japan, 2010, pp. 574–580.
[94] Y. Ohnuma and J. Itoh, "A single-phase-to-three-phase power converter with an active buffer and a charge circuit," *IEEJ J. Ind. Appl.*, vol. 1, no. 1, pp. 46–54, Jul. 2012.
[95] Y. Ohnuma and J. I. Itoh, "Control strategy for a three-phase to single-phase power converter using an active buffer with a small capacitor," in *Proc. IEEE Int. Power Electron. Motion Control Conf.*, Wuhan, China, 2009, pp. 1030–1035.
[96] M. Chen, K. K. Afridi, and D. J. Perreault, "Stacked switched capacitor energy buffer architecture," *IEEE Trans. Power. Electron.*, vol. 28, no. 11, pp. 5183–5195, Nov. 2013.
[97] K. K. Afridi, M. Chen, and D. J. Perreault, "Enhanced bipolar stacked switched capacitor energy buffers," *IEEE Trans. Ind. Appl.*, vol. 50, no. 2, pp. 1141–1149, Mar./Apr. 2014.

Yao Sun (M'13) was born in Hunan, China, in 1981. He received the B.S., M.S., and Ph.D. degrees from the School of Information Science and Engineering, Central South University, Changsha, China, in 2004, 2007, and 2010, respectively.

He has been an Associate Professor at the School of Information Science and Engineering, Central South University. His research interests include matrix converter, microgrid, and wind energy conversion system.

Yonglu Liu was born in Chongqing, China, in 1989. He received the B.S. and M.S. degrees in electrical engineering from Central South University, Changsha, China, in 2012 and 2015, respectively, where he is currently working toward the Ph.D. degree in electrical engineering.

His research interests include matrix converter and ac/dc converter.

Mei Su was born in Hunan, China, in 1967. She received the B.S., M.S., and Ph.D. degrees from the School of Information Science and Engineering, Central South University, Changsha, China, in 1989, 1992, and 2005, respectively.

Since 2006, she has been a Professor at the School of Information Science and Engineering, Central South University. Her research interests include matrix converter, adjustable speed drives, and wind energy conversion system.

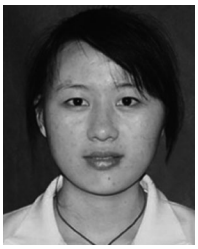

Wenjing Xiong was born in Hunan, China, in 1991. She received the B.S. degree in automation from Central South University, Changsha, China, in 2012, where she is currently working toward the Ph.D. degree in electrical engineering.

Her research interests include power electronics and power transmission.

Jian Yang (M'09) received the Ph.D. degree in electrical engineering from the University of Central Florida, Orlando, FL, USA, in 2008.

He was a Senior Electrical Engineer with Delta Tau Data Systems, Inc., Los Angeles, CA, USA, from 2007 to 2010. Since 2011, he has been with Central South University, Changsha, China, where he is currently an Associate Professor at the School of Information Science and Engineering. His main research interests include control application, motion planning, and power electronics.